Supplemental Methods

Genetic analysis. Genomic DNA was extracted from EDTA-blood probes using standard procedures. The following primers were used to amplify all 10 exons of the SLC2A1 gene:

exons	5` - 3`	3` - 5`
1	GAGTCAGAGTCGCAGTGGGAG	GCGTAAGGCGGGCAGGAGTC
2	GAAAGACTGGTGGTGCCAAGAG	GACAGTACAGTGCGTTCATATAAATGACTCT
3+4	GGCGGGGCTCTCAGATGAACTCCA	CTGGACCTGTGTACCATAGTTGTCCTCTGC
5+6	TCCCATGTGACCGATGAGGAAACTGAGA	TTCGGCAGAGGCGTATCTGTTGTTTCA
7+8	CCTGGGTCCC ACATCCACTGCTA	GGAGGAGCAAGTTCAAGAGAGGATGTGT
9+10	CCTGAGGATCCATCACAACCCAGTCTAACTTTT	TGAATATTCTTCTGGACATCATTGCTGGCTG

Amplification of the DNA was performed by the polymerase chain reaction (PCR) with the following conditions in a final volume of 50 µl: 50 ng DNA, 30 pmol of each primer, 15 mM of each dNTP, 5 µl Buffer (500 mM KCl, 200 mM TrisHCl, 25 mM $MgCl_2$, 0.01% gelatine, pH 8.4), 0.2 µl Taq polymerase (Pharmacia Biotech). Samples were amplified in a thermocycler (Whatman Biometra) using the following conditions: 95°C for 3 min; 35 cycles of 30 s at 95°C, 45 s for annealing and 30 s at 72°C; followed by a final extension period of 2 min at 72°C. PCR products were sequenced at GATC Biotech. For further mutational analysis, in particular to exclude the mutations in normal controls, we used three different restriction digestions (enzymes from Biolabs). Exon 6 and 7 were amplified as described above and digested over 2 hours at 37°C. In case of the Q282_S285del mutation, exon 6 was digested by AlwNI; the site was removed by the mutation so that an additional band of 636 base pairs (bp) appeared in heterozygous patients carrying one mutant and one WT allele when compared to controls carrying two WT alleles. A MspI site in exon 7 was removed by the G1119A mutation and an additional band of 388 base pairs (bp) appeared. A HpyCH4III site was newly created by the G1002A mutation in exon 6 and two additional bands of 147 and 578 bp appeared in case of the mutation. Multiplex ligation-dependent probe amplification (MLPA) was performed using a standard kit (P138 SLC2A1, MRC Holland).

Mutagenesis and RNA preparation. A plasmid with the cDNA of *SCL2A1* in the expression vector pSP65 was kindly provided by Dr. Mike Mueckler (1). The mutagenesis to introduce the Q282_S285del deletion was performed using an overlap PCR strategy with primers given below, and the final PCR fragment was reassembled in pSP65.

PCR1	5`-GAAGCTCAGAATAAACGCTCAACTT-3`
	5`-ATCCTCATCGCTGTGGTGCTGCAGCTGTCTGGCATCAA-3`
PCR2	5`-TTGATGCCAGACAGCTGCAGCACCACA-GCGATGAGGAT-3`
	5`-GTTCTTGAGGCTGGTTTAGTGGAT-3`
PCR3	5`-GAAGCTCAGAATAAACGCTCAACTT-3`
	5`-GTTCTTGAGGCTGGTTTAGTGGAT-3`

The QuickChange site-directed mutagenesis kit (Stratagene) was used to introduce the single base pair exchanges c.G823A and c.G940A into the *SCL2A1* cDNA, resulting in A275T and G314S amino acid exchanges, respectively. Primers were as follows:

A275T	5`-GCCAGCCCATCCTCATCACTGTGGTGCTGCAGCTG-3`
	5`-CAGCTGCAGCACCACAGTGATGAGGATGGGCTGGC-3`
G314S	5`-GCCACCATTGGCTCCAGTATCGTCAACACGG-3`
	5`-CCGTGTTGACGATACTGGAGCCAATGGTGGC-3`

All mutations were verified by restriction digestion and sequencing. Plasmids carrying WT or mutant cDNA were linearized using digestion with Sal I (Biolabs). Linearized plasmids served as templates for *in vitro* transcription using the Sp6 mMessagemMachine kit (Ambion).

Oocyte preparation and injection. All procedures were approved by the Regierungspraesidium Tuebingen, Germany. Female *Xenopus laevis* frogs were anesthetized with Tricaine (0.1%; Sigma) and placed on ice to maintain anesthesia. Oocytes were surgically removed and immediately treated for two hours with collagenase (2 mg/ml of type CLS III collagenase, Biochrom AG) in OR2-solution (in mM: 82.5 NaCl, 2.5 KCl, 1 $MgCl_2$ and 5 Hepes, pH 7.6) to remove follicular cells. Defolliculated oocytes were stored at 16°C in modified Barth's solution (mM: 88 NaCl, 1 KCl, 2.4 $NaHCO_3$, 0.82 $MgS0_4$, 0.33 $Ca(N0_3)_2$, 0.41 $CaCl_2$, 10 Hepes and 30 I.U./ml of gentamicinsulphate (Biochrom AG), pH 7.4). Diluted cRNA (30-60ng) was injected into each oocyte within 24 h of preparation. For all experiments, oocytes were injected by equal amounts of WT or mutant cRNA, as was confirmed by both spectrophotometry (Ultrospec3000, GE Healthcare) and band intensity on an agarose gel before the injection.

Glucose uptake experiments in oocytes. Oocytes injected with mutant or WT cRNA of GLUT1 transporters were kept in modified Barth's solution (see above) at 16°C for 72 hours. Zero-trans influx experiments with 3-O-methyl-D-glucose were performed similarly as described previously (2). For each experiment, ten oocytes were incubated for 5 min in 200 µl modified Barth's solution containing a constant amount (1.2 µCi) of 3-0-[3H]methyl-D-glucose (Amersham Biosciences) and 1 to 50 mM unlabeled 3-O-methyl-D-glucose (Sigma). The osmolarity was kept constant at 237 mOsm/l by adding sucrose as necessary. After incubation, the influx was stopped by washing four times with 1.5 ml ice-cold Barth's solution containing 0.2 mM phloretin. In a separate set of experiments, we confirmed that within the 5 min incubation time the uptake increased linearly with time. After the final wash the oocytes were transferred to 0.1 ml H_2O and lysed mechanically. The solution was centrifuged at 250 g for 2 min. The supernatant was mixed with 4.9 ml of scintillation fluid Gold (Amersham Biosciences) and radioactivity measured using a scintillation counter (Tri-Carb 2200CA, Packard/PerkinElmer). For each experimental day, three experiments for each glucose concentration were averaged for both mutant and WT transporters. Water-injected oocytes served as controls to record the background activity.

For kinetic analysis, glucose uptake raw data (in pmol/oocyte/min) obtained in oocytes for different concentrations of 3-O-methyl-D-glucose (OMG) were transformed according to Lineweaver-Burk. The linear function: $1/V\ (1/[S]) = 1/V_{max} + K_m/V_{max}*1/[S]$
was fit to the data points, with [S] being the concentration of OMG, V the uptake velocity in pmol/oocyte/min obtained for a given [S], V_{max} the maximal uptake velocity reflecting the maximal transport capacity of GLUT1, and K_m the Michaelis-Menten constant representing the concentration [S] for which the half-maximal uptake velocity ($V_{1/2}$) is reached. In this data representation, the y-axis intercept of the graph equals $1/V_{max}$ and the x-axis intercept represents $-1/K_m$.

Glucose uptake in erythrocytes. Fresh blood samples (5 ml) were immediately mixed with the same amount of isotonic NaCl solution containing 10 units of heparin per ml and were drawn from patients and controls on the same day and shipped overnight to our laboratory. All following procedures were performed at 4°C. The probes were centrifuged at 2500 g for 10 min. Pellets of 2 ml were washed three times in PBS (137 mmol/l NaCl, 2.7 mmol/l KCl, 4.3 mmol/l Na_2HPO_4, 1.4 mmol/l KH_2PO_4, pH 7.4) and then resuspended in 5 ml PBS. Aliquots of 100 µl of this suspension were mixed with 200 µl of radioactive solution (0.5 µCi/ml 3-O-(^{14}C-Methyl)-D-glucose (OMG, Sigma) in PBS). The glucose uptake was stopped after 0, 10,

20 or 30 s, or after 25 min (equilibrium) by adding 1 ml of ice-cold stop solution (100 µmol/l HgCl and 50 µmol/l phloretin, Sigma) followed by a centrifugation at 250 g for 5 min and two additional washing steps in 500 µl of stop solution with respective centrifugations. The erythrocytes were then lysed by adding 500 µl of 3.1% trichloracetic acid (Sigma). The supernatant was mixed with 4.5 ml of scintillation fluid Gold and the radioactivity was measured using a scintillation counter.

For data analysis, the value measured at 0 s, i.e. when the radioactivity and stop solution were added at the same time to the erythrocyte suspension, was defined as the background and subtracted from all other values. Three measurements were obtained for each time point and the average was taken for further analysis. The logarithm $\ln(1-c_t/c_{eq})$, with c_t being the assimilated radioactivity after time t and c_{eq} the radioactivity in the equilibrium, was plotted against time and a linear function was fit to the data points for each charge of erythrocytes.

Western blot analysis of GLUT1 expressed in oocytes. Oocytes injected with equal amounts of mutant or WT cRNA of GLUT1 kept in modified Barth's solution at 16°C for 48 hours. 10 oocytes of each group were homogenized in 100 µl of lysis buffer containing 250 mM saccharose, 0.5 mM EDTA, 5 mM Tris-HCl (pH 7.4), 1 mM PMSF, 2 µg/ml Aprotinin and 2 µg/ml Pepstatin (Sigma-Aldrich), followed by three low speed centrifugations. Proteins of the resulting supernatant were separated by SDS polyacrylamide gel electrophoresis (12 % polyacrylamide) and transferred onto a PVDF membrane. Blots were blocked in 3% nonfat milk and probed with primary (rabbit anti-GLUT1, Abcam) and secondary (horseradish peroxidase goat anti-rabbit, Cell Signaling Technology) antibodies in 1:100 and 1:1000 dilutions, respectively. Antibody binding was detected with the enhanced chemoluminescence (ECL) kit from Amersham (GE Healthcare). The same membrane was stripped and reprobed with an anti alpha-tubulin antibody (1:2000, Milipore), used as a loading control.

Immunocytochemical analysis of GLUT1 expression in oocytes. Oocytes were injected and kept in modified Barth's solution as for western blots. Fixation was first performed in 4% paraformaldehyde with 15% saccharose for 15 min followed by incubation in methanol for another 15 min at RT. Fixed oocytes were then frozen in tissue protecting medium (Leica) in fluid nitrogen vapour and sectioned on a cryotome (thickness 14 µm, Leica). Sections were mounted on BSA-treated slides and dryed overnight. For staining, the sections were blocked in PBS containing 0.2% Triton, 2% BSA and 5% milk. The incubation with the anti-GLUT1

(1:100) antibody was performed in the blocking solution over night at 4°C. After extensive washing, detection was performed using a fluorescently labelled secondary antibody (Alexa Fluor 488, Invitrogen). Sections were then covered with a mounting medium (Vecta Shield, Vector Laboratories) and examined using an Axioscope 2 plus microscope (Zeiss).

Further details for the determination of $[Na^+]_i$ and $[K^+]_i$ in oocytes. The calibration curves were generated by fitting the obtained data points with a Nikolsky-Eisenmann function (3) according to the following equation: $E([X]) = E_0 + (RT/zF)*\log([X] + k*(150-[X]))$,
with E being the recorded ion-selective potential, [X] the Na^+ or K^+ concentration, E_0 the offset potential and k the selectivity coefficient. (RT/zF) is the slope of the calibration curve with R being the universal gas constant, T the absolute temperature in Kelvin, z the ionic valence, and F Faraday's constant.

Resting membrane potentials (RMPs) of oocytes were determined with conventional electrodes using a Turbo TEC01C amplifier (npi electronic GmbH). After insertion of the ion selective electrode (ISE), which was connected to an Axopatch 200B amplifier (Axon Instruments), ion-selective potentials were calculated as the difference between the potentials of both electrodes. The intracellular ion concentrations were determined using the respective calibration curves, as shown below:

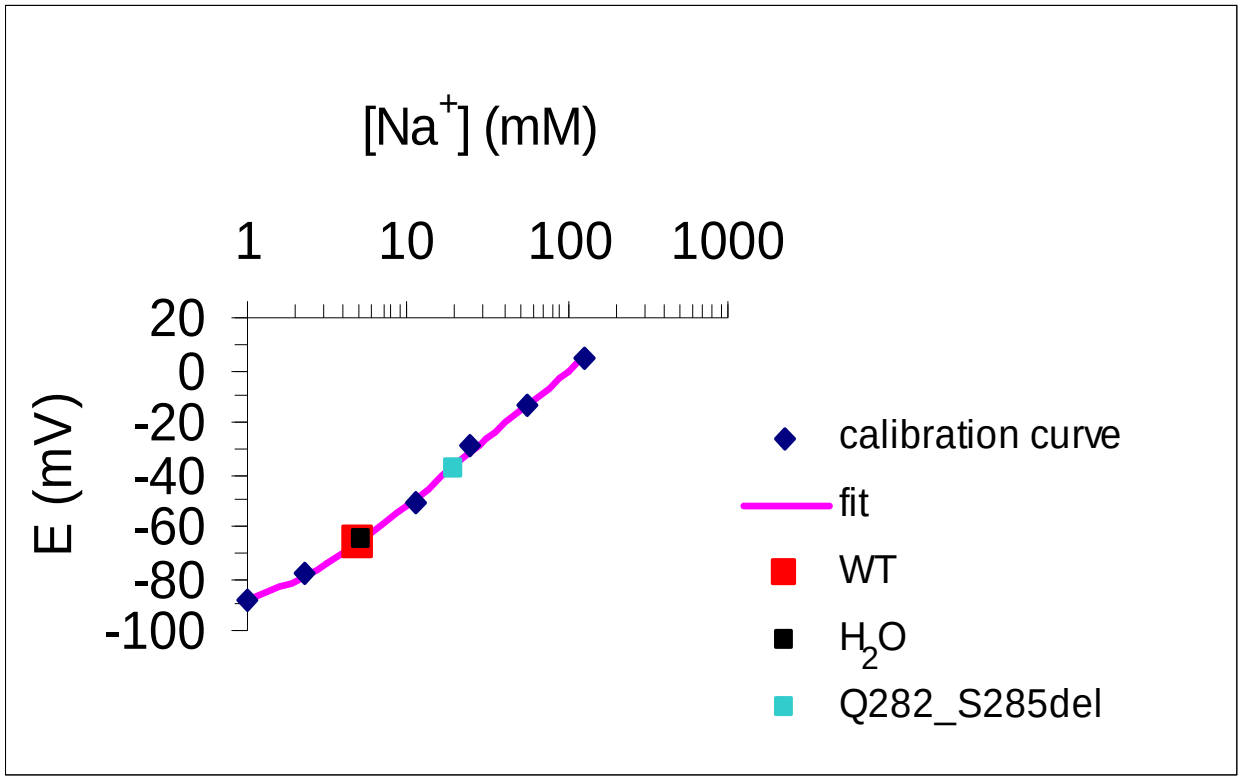

	WT ISE-P	WT RMP	Offset	Q282_S285del ISE-P	Q282_S285del RMP	Offset	H_20 ISE-P	H_20 RMP	Offset
	-69	-54	1 0	-38	-23	0 0	-60	-53	1 1
	-65	-45	0 0	-42	-18	3 -1	-69	-49	0 0
	-68	-47	1 0	-36	-17	1 0	-69	-31	1 0
	-58	-27	1 0	-37	-20	2 0	-67	-46	0 0
	-65	-42	2 0	-40	-15	3 0	-65	-46	1 0
	-70	-42	1 0	-34	-15	2 0	-63	-36	1 0
MW	-66	-43		-38	-18		-66	-44	
SD	4	9		3	3		4	8	
SEM	2	4		1	1		1	3	

Graph on previous page: Example of a calibration curve fit by a Nikolsky-Eisenmann function and the calculated intracellular ionic concentrations shown for the experiment presented in Figure 3C of the main text. The slope (RT/zF) was 54.6 mV, the selectivity coefficient was 0.0093.

The table gives the primary data (potentials in mV) obtained with the ion selective electrode (ISE-P = potential recorded with ISE) and the standard electrode (RMP = resting membrane potential) for 3 groups of 6 oocytes each injected with either WT or Q282_S285del cRNA, or water. The offset of both electrodes was set to zero in the bath solution before impaling the oocytes and was evaluated for stability after each recording. Offset values for both electrodes, recorded after each experiment, are given in mV for each condition.

Determination of the input resistance of oocytes. Oocytes were injected as described above and were kept in modified Barth's solution (in mM: 85 NaCl, 1 KCl, 2.4 $NaHCO_3$, 0.82 $MgSO_4$, 0.33 $Ca(NO_3)_2$, 0.41 $CaCl_2$, 10 Hepes, 4.5 NaOH, pH 7.4) supplemented with 30 IU/ml of gentamicinsulphate (Biochrom AG). Recordings were performed in parallel in a blinded and alternating manner for oocytes injected with mutant or WT cRNA or water, 2-3 days after injection. We used standard two-electrode voltage clamping with a Turbo TEC01C amplifier (npi electronic GmbH). Electrodes were filled with 3 M KCl and had a resistance of <1 MOhm. Resting membrane potentials (RMPs) of oocytes were determined before insertion of the current electrode. Oocytes were clamped to a holding potential of -80 mV and the leak current was determined. The input resistance of the oocytes was calculated according to Ohm's law.

$^{86}Rb^+$ flux experiments in Xenopus laevis oocytes. Oocytes were prepared as described above and injected with equal amounts of mutant or WT cRNA of GLUT1 transporters. The injected oocytes were kept in modified Barth's solution (in mM: 85 NaCl, 1 KCl, 2.4 $NaHCO_3$, 0.82 $MgSO_4$, 0.33 $Ca(NO_3)_2$, 0.41 $CaCl_2$, 10 Hepes, 4.5 NaOH, pH 7.4) for 2 days at 16°C with 50µg/ml gentamycin sulphate (Biochrom AG). All procedures were performed on ice. The uptake measurements were started by adding 2.5 µCi of $^{86}Rb^+$ (GE Healthcare) in 200 µl MBS plus ouabain and bumetanide (0.1 mM each) and stopped by washing five times without isotope after 2 h of incubation. Oocytes were dissolved in 0.5 ml of 1% SDS, disrupted mechanically and centrifuged at 250 g for 5 min. The supernatant was mixed with 4.5 ml scintillation fluid Gold (Amersham) and the radioactivity measured in a scintillation counter.

$^{86}Rb^+$ flux experiments in erythrocytes. Fresh blood samples (5 ml) were immediately mixed with the same amount of isotonic NaCl solution containing 10 units of heparin per ml and were drawn from patients and controls on the same day and shipped overnight to our laboratory. All procedures were performed on ice. A 2-ml erythrocyte pellet was washed three times in MOPS (mM: 150 NaCl, 15 MOPS, 5 glucose, pH 7.4) and finally resuspended in 5 ml MOPS containing 0.1 mM bumetamide and ouabain each. 1.2 µCi of $^{86}Rb^+$ was added to 100 µl of the erythrocyte suspension and incubated for 2 h followed by 4 times washing in a buffer (mM: 106 MgCl2, 10mM Tris-Cl, pH 7.4). The cells were lyzed using 500 µl of 3.1% of trichloric acid and the supernatant after centrifugation at 250 g for 5 min was mixed with 4.5 ml of scintillation fluid Gold. The radioactivity was measured using a scintillation counter.

Further experiments using erythrocytes from patients and normal controls. EDTA blood samples from three patients of family PED1 (III-2, IV-1, IV-2) and of three normal controls were drawn on the same day and shipped to our laboratory overnight. For the experiments with native erythrocytes described in the following paragraphs, data from all three patients (patch-clamp, fluo3 fluorescence, hemolysis) and three controls (fluo3 fluorescence, hemolysis) or from two patients (forward scatter, annexin V binding) and two controls (patch-clamp, forward scatter, annexin V binding) were pooled for data analysis.

Breakdown of the phospholipid asymmetry and cell volume. Erythrocytes were incubated for 24 h at 37°C in Ca^{2+}-containing NaCl solution. Thereafter, cells were washed and stained (20 min at room temperature) with Annexin-Fluos (Boehringer Mannheim**;** 1:500 dilution**)** in annexin-binding buffer (containing in mM: 125 NaCl, 10 Hepes, 5 $CaCl_2$, titrated

with NaOH to pH 7.4). Forward scatter (as a measure of cell size/volume) and annexin V fluorescence binding (as a measure of phosphatidylserine exposure) was determined by flow cytometry using fluorescence channel FL-1.

Erythrocyte calpain activation. Blood was washed 3 times in Ca^{2+}-containing NaCl solution and stored at 4°C to eliminate the white cells. As a positive control, erythrocytes were exposed to 1 µM of the calcium ionophore ionomycin for 30 min at 37°C. The other erythrocyte samples were incubated (24 h at 37°C) in Ca^{2+}-containing NaCl, pelleted, and 200 µl of the pellet was hemolysed by hypotonic shock in a 20 mM Hepes-containing cocktail of protease inhibitors (pH 7.4) (Roche). Ghosts were pelleted (15,000 g for 20 min at 4°C) and lysed in a buffer containing (in mM: 125 NaCl, 25 Hepes/NaOH pH 7.3, 10 EDTA, 10 Na-pyrophosphate, 10 NaF, 0.1% SDS, 0.5% deoxycholic acid, 1% triton-X, 0.4% β-mercaptoethanol).

Lysates were separated by 10% SDS-PAGE (50 µg protein per lane) and transferred electrophoretically to Protan BA83 nitrocellulose membranes (Schleicher and Schuell). Protein transfer was controlled by Ponceau red staining. After blocking the non-specific sites with 5% nonfat milk, the blots were probed overnight at 4°C with a polyclonal rabbit anti-human µ-calpain (large subunit) antibody (Cell Signaling Technology) diluted at 1:500. After washing, the blots were incubated for 1 h at 21°C with a secondary goat anti-rabbit antibody (Cell Signaling Technology) conjugated with horseradish peroxidase at a 1:1000 dilution. Antibody binding was detected with the enhanced chemoluminescence (ECL) kit (Amersham).

Hemolysis. Erythrocytes were washed and incubated 24 h at 37°C in Ca^{2+}-containing NaCl solution. Incubation was stopped by centrifugation and the supernatants were harvested. As a measure of hemolysis the hemoglobin (Hb) concentration of the supernatant was determined photometrically upon transforming the Hb into *cyanomet*Hb. Formation of *cyanomet*Hb was accomplished by adding 0.8 mM KCN, 0.61 mM $K_3[Fe(CN)_6]$, 1 mM KH_2PO_4, and 0.5% Extran to the supernatants (550 µl per 200 µl sample).

Fluorine-18 2-fluoro-2-deoxy-D-glucose positron emission tomography (FDG-PET). Patients were fasted 6-8 hours before FDG-PET scanning (Siemens ECAT HR+). Blood glucose level was below 120 mg%. Prior to i.v. application of 160-195 MBq FDG, a transmission scan for measured attenuation using a 68 Ge/68 Ga rotating source (cold transmission) was acquired. Patients were positioned comfortably on the scanner table 30 min prior to the i.v. administration of FDG. The PET scanner room was quiet and dimly lit and patients were

instructed not to speak, read or otherwise be active. Then an FDG uptake phase of 20 min was followed by acquisition of a 15 min emission scan in 3-D-mode. After scatter correction data were iteratively reconstructed based on the measured attenuation corrected images. For evaluation of the individual regions showing a relative hypometabolism, statistical parametric mapping (SPM99, Wellcome Department of Imaging Neuroscience Group, London, UK; http://www.fil.ion.ucl.ac.uk/spm) was implemented. Data were normalized into a standard stereotaxic space of Talairach and Tournoux and then compared to a group of normal controls (n=17; mean age 37 years, range 19-52) by means of a T-test. A group comparison was performed with p=0.05 using correction for multiple comparisons. Additionally, a single subject analysis was performed for each subject with p=0.001 without correction for multiple comparisons.

Magnetic resonance imaging (MRI). Cranial MRI scanning was performed on a 1.5 Tesla scanner (Magnetom Vision, Siemens) for all affected members of family PED1 and the index patient of PED5. The scanning protocol included axial T1- (repetition time 532 ms, echo time 17 ms, slice thickness 5 mm), T2- (repetition time 2475 ms, echo time 102 ms, slice thickness 5 mm), T2*- (repetition time 2000, echo time 30 ms, slice thickness 5 mm) -weighted and fluid attenuated inversion recovery (FLAIR: repetition time 9000 ms, echo time 110 ms, slice thickness 5 mm) sequences.

Molecular modelling. We started the modelling using the coordinates of a published GLUT1 model (4). In this model, the residues QQLS282-285 were deleted as predicted by the c.1022-1033del mutation and the backbone was religated by a series of energy minimisations *in vacuo* using force fields AMBER and Gromos96 implemented in BALLview 1.1.1 and DeepView / Swiss-PDB viewer v3.7. To analyze the resulting changes in the geometry of the central tunnel further, we utilised CAVER. CAVER traverses points in an empty space of a tunnel and prefers those points that have more empty space around. This is technically done by protein grid approximation and evaluating cost function for a minimum. Cost function gives a penalty to points that are close to protein atoms, i.e. preferable points have a small value.

References to Supplemental Methods

1. Mueckler, M., Caruso, C., Baldwin, S.A., Panico, M., Blench, I., Morris, H.R., Allard, W.J., Lienhard, G.E., and Lodish, H.F. 1985. Sequence and structure of a human glucose transporter. *Science* **229**:941-945.
2. Brockmann, K., Wang, D., Korenke, C.G., von Moers, A., Ho, Y.Y., Pascual, J.M., Kuang, K., Yang, H., Ma, L., Kranz-Eble, P., et al. 2001. Autosomal dominant glut-1 deficiency syndrome and familial epilepsy. *Ann. Neurol.* **50**:476-485.
3. Fry, C.H., Hall, S.K., Blatter, L.A., and McGuigan, J.A. 1990. Analysis and presentation of intracellular measurements obtained with ion-selective microelectrodes. *Exp. Physiol.* **75**:187-198.
4. Salas-Burgos, A., Iserovich, P., Zuniga, F., Vera, J.C., and Fischbarg, J. 2004. Predicting the three-dimensional structure of the human facilitative glucose transporter glut1 by a novel evolutionary homology strategy: insights on the molecular mechanism of substrate migration, and binding sites for glucose and inhibitory molecules. *Biophys. J.* **87**:2990-2999.

Supplemental Table 1. Laboratory results of family PED1 (pathological results are marked in grey).

Parameter	Unit	Normal range[a]	Individual[b]			
			II.2	III.2	IV.1	IV.2
Hematology						
Hemoglobin	g/l	130-180	130	135-139	108-150	109-132
Hematocrit	l/l	0.40-0.52	0.40	0.40	0.35	0.31
Reticulocytes	$x10^{-3}$	5-15	-	114-180	98-142	121
MCV	fl	76-98	102	99-104	90-107	88-104
MCH	pg	27-34	35.1	35.2	30.0-40.5	30.9-35.0
MCHC	g/l	310-360	343	355	353-380	334-373
Thrombocytes	g/l	150-450	132	207-294	255	342
Erythrocytes (RBC)	T/l	4.4-5.7	3.7	3.8-3.9	3.78	3.56
McLeod phenotype (absence of XK protein)	-	Absent	absent	absent	-	-
RBC membrane analyses[c]						
Membrane protein electrophoresis	-	Normal	normal	normal	Normal	-
Spectrin	$x10^3$ molecules/cell	200-250	225	210	212	-
Ankyrin	$x10^3$ molecules/cell	100-150	102	108	115	-
Band 3	$x10^3$ molecules/cell	700-1,500	1,200	900	1,050	-
Lipid phosphor content	$x10^{16}$ mol/cell	2.9-4.2	4.0	3.6	3.6	-
RBC enzyme activities						
Glutathion metabolism[d]		-	-	normal	Normal	-
Glucose and glycogen metabolism[e]		-	-	normal	Normal	-
RBC energy parameters[f]						
ATP	nmol/ml	1096-1460	1321	1203	-	-
ADP	nmol/ml	119-235	187	188	-	-
AMP	nmol/ml	4.8-21.4	20.6	21.2	-	-
$NADP^+$	nmol/ml	4.3-21.9	13.8	8.5		-
NADPH	nmol/ml	8.2-20.2	15.3	20.0	-	-
NAD^+	nmol/ml	22.0-37.6	27.1	30.3	-	-
NADH	nmol/ml	11.1-25.5	17.9	22.6	-	-
ATP/ADP	nmol/ml	5.8-9.8	7.1	6.4	-	-
ATP/AMP	nmol/ml	62-170	64	57	-	-
Energy load ([ATP]+½[ADP] / [ATP]+[ADP]+[AMP])		0.90-0.96	0.93	0.92	-	-

Supplemental Table 1 (continued)

Parameter	Unit	Normal range[a]	Individual[b]			
			II.2	III.2	IV.1	IV.2
Serum						
Na^+	mmol/l	132-154	141	139	normal	137
K^+	mmol/l	3.5-5.4	4.21	4.35	normal	4.93
Iron	µmol/l	9.5-29.9	-	24.8	normal	-
Ferritin	µg/ml	35-217	-	770-923	normal	-
Haptoglobin	g/l	0.30-2.05	0.08	0.08-0.1	< 0.1-0.2	< 0.1
Creatinine	µmol/l	50-110	75	71	normal	-
Urea	mmol/l	1.7-8.3	5.5	4.2	7	-
Bilirubin	µmol/l	0-17	52.3	65.1	22.9	24.1-27.0
AST	U/l	0-19	30	22	normal	-
ALT	U/l	0-23	55	51	normal	-
GGT	U/l	6-28	20	14	normal	-
Lactate	mmol/l	1.1-2.1	1.47	1.78	1.10	-
Creatine kinase	U/l	0-80	50	20	normal	-
C-peptide	nmol/l	0.33-1.2	1.5	0.39	-	-
Lactate dehydrogenase	U/l	< 240	238	166	198	235-367
Pyruvat	mg/l	3.6-5.9	-	-	6.4	-
Lactate dehydrogenase isoenzymes	-	-	normal	normal	-	-
Cerebrospinal fluid (CSF)						
Cell count	n/µl	< 5	0	0	0-1	0
Na^+	mmol/l	139-151	145	149	-	-
K^+	mmol/l	2.46-3.48	3.14	2.74	-	-
Lactate	mmol/l	1.2-2.1	1.39	0.75	0.8-1.0	0.8
Protein	mg/l	200-450	435	483-630	310	-
Glucose	mmol/l	2.7-4.2	2.49	2.13	2.4-2.7	2.5
CSF-serum glucose ratio		0.62-0.68	0.48	0.39	0.47-0.5	0.55
Pyruvate	mg/l	0.5-1.7	-	-	1.9	-
Biogenic amines	-	-	-	normal	-	-

[a] The displayed normal ranges include those from all laboratories used in the present study, but do represent only ranges for adults. Pathological results in grey are judged according to the normal values for the correct age and laboratory, respectively, if at least one value obtained during the observation period was outside the normal range.

[b] If repetitive analyses were performed, the obtained range of laboratory results is displayed.

[c] RBC membrane analyses were performed using standard methods. Normal values were defined in 40 healthy control probands.

[d] Enzyme activities were determined for glutathion peroxidase and glutathion reductase.

[e] Enzyme activities were determined for glucose-6-phosphate-dehydrogenase, 6-phospho-gluconate-dehydrogenase, hexokinase, phospho-glucomutase, glucose-phosphate-isomerase, phosphor-fructokinase, aldolase, triose-phosphate-isomerase, glyceraldehyde-3-phosphate-dehydrogenase, 2,3-diphospho-glycerate-mutase, 3-phospho-glycerate-1-kinase, mono-phospho-glycerate-mutase, enolase, pyruvate kinase, lactate dehydrogenase, and adenylate kinase.

[f] RBC energy parameters were determined as described in Wynants J and van Belle, H. Analytical Biochemistry 1985;144:258-266.

All other hematology, erythrocyte enzyme activity, serum and CSF parameters were measured using standard clinical chemistry methods. RBCs: red blood cells.

Supplemental Table 2. Intracellular sodium ($[Na^+]_i$) and potassium ($[K^+]_i$) concentrations determined in erythrocytes from 3 patients and 2 normal controls after incubation with 0 or 15 mM glucose for two hours, respectively.

	0 mM glucose		15 mM glucose	
	$[Na^+]_i$ (mM)	$[K^+]_i$ (mM)	$[Na^+]_i$ (mM)	$[K^+]_i$ (mM)
Patients	37	49	35	52
	29	56	28	62
	35	50	28	54
Controls	8.3	79	8.2	79
	4.9	89	5.4	88

Legend to Supplemental Video

The video shows several episodes of dyskinesias of the index patient (III-2) of family PED1. *After 20 min. of exercise:* The patient has been sitting on an ergometer for 20 min. cycling with a constant power of 150 W. At this time he experiences involuntary dystonic and hyperkinetic movements causing coordination problems, as can be seen in the video. When he stopped exercising, the dyskinesias stopped as well in this case.

Dyskinesias after exercise: After another, similar period of exercising on a bicycle ergometer, the patient experienced heavy ongoing spontaneous dyskinesias at rest for about 1 hour. It can be observed that also these dyskinesias were restricted to the exercised lower limbs, but involved both proximal and distal muscle groups resulting in ballistic, dystonic and choreoathetotic movements.

The next three sequences are earlier home videos of the same patient taken by his wife:

Dystonic gait after walking: After a longer period of walking (approximately 1 hour), the patient showed a dystonic gait. These dyskinesias ceased when he stopped walking.

Dyskinesias of the upper extremities: After painting his flat, the patient experienced spontaneous dyskinesias of the exercised upper limbs.

Generalized dyskinesias: Very rarely, the patient also showed dramatic periods of such heavy generalized dyskinesias.

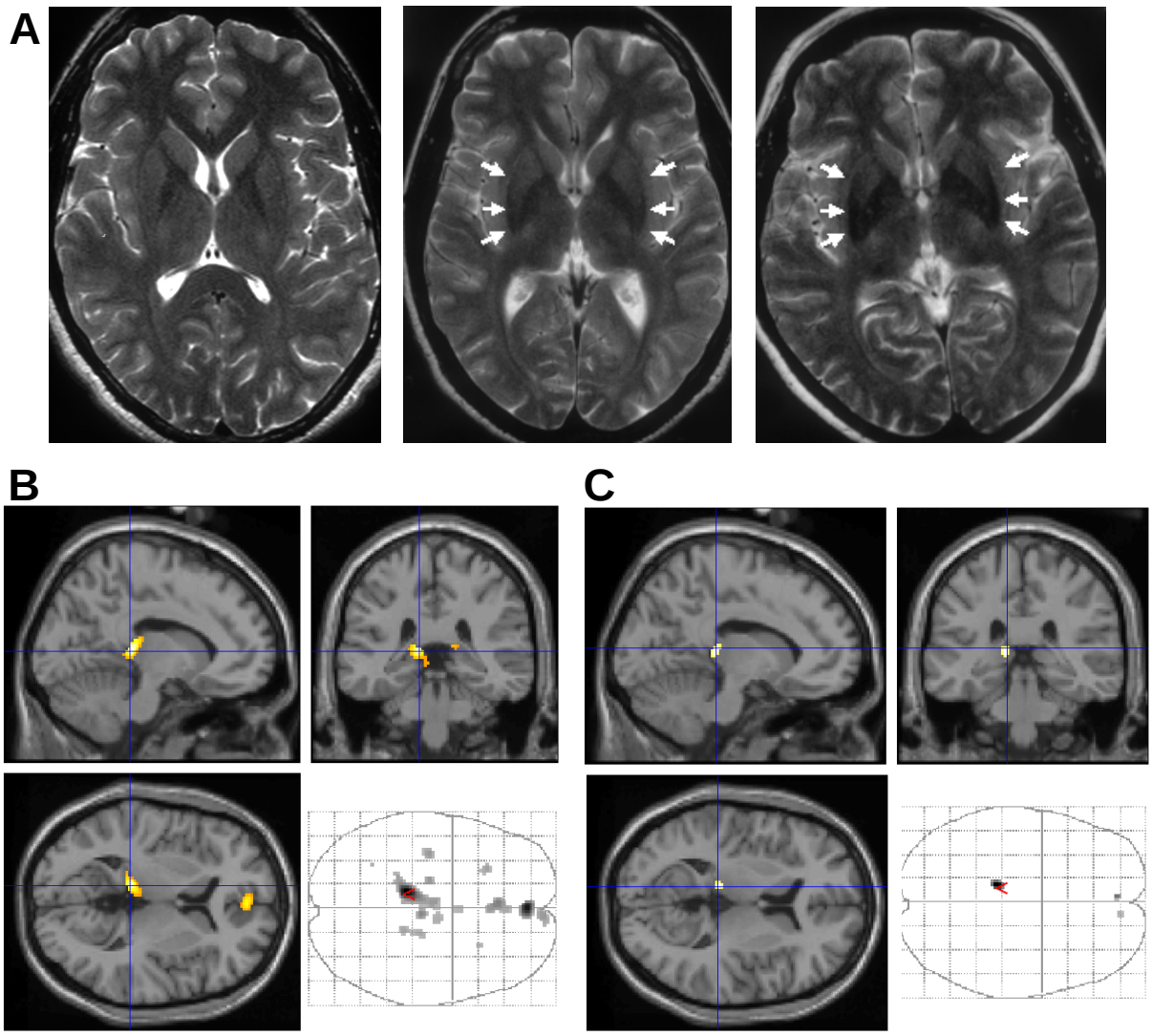

Figure S1. Brain imaging. (**A**) T2-weighted magnetic resonance imaging (MRI) of a normal control aged 43 years (left), patient III-2 (family PED1) at the age of 33 years (middle), and patient II-2 (PED1) at the age of 53 years (right). Lower signal intensities were found for both patients in the dorsolateral putamen (white arrows). (**B**) FDG-PET of the index case (PED1, III-2) when compared to 17 age-matched normal controls using statistical parametric mapping (SPM99); p=0.001, without correction for multiple comparisons. Shown is the relative hypometabolism in the left>>right thalamus. The glass brain view does not reveal major other sites of metabolic changes. (**C**) FDG-PET of II-2, III-2 (PED1) and the index case of family PED5 compared to 17 age-matched normal controls; p=0.05, corrected for multiple comparisons. All three individuals are right-handed and had classical PED alone (no evidence for epilepsy or mental retardation). There is a significant hypometabolism in the left thalamus. (**D**) Relative hypermetabolism in the putamen when FDG-PETs of II-2, III-2 (PED1) and the index case of family PED5 are compared to 17 normal controls; p=0.001, without correction for multiple comparisons. The right side of the image shows the right side of the brain in case of PET images B-D.

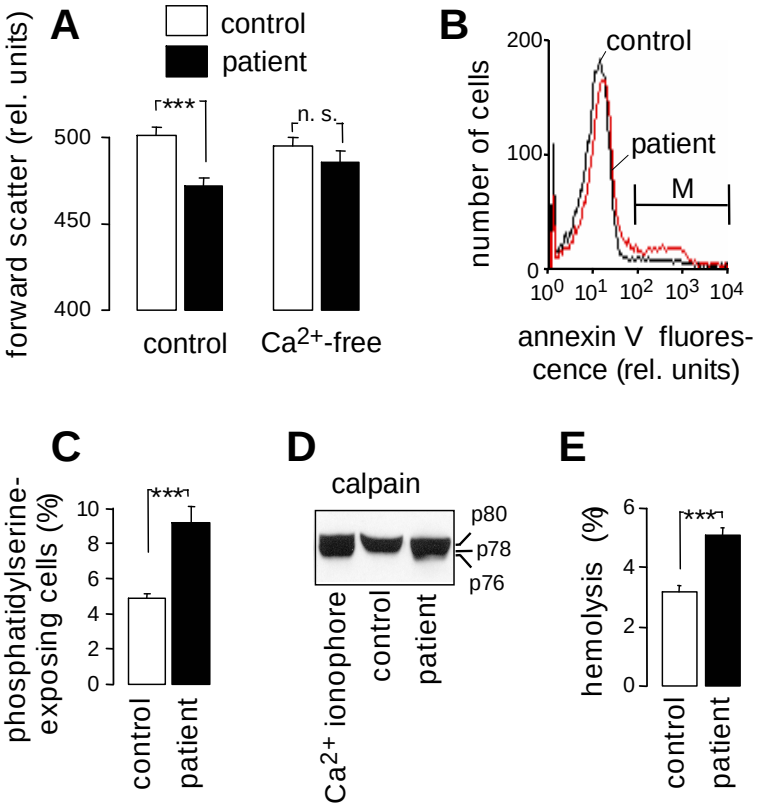

Figure S2. Functional analysis of suicidal death of erythrocytes from patients of family PED1 compared to controls. (**A**) Mean forward scatter (±SEM; n=7-10) as a measure of cell size/volume recorded by flow cytometry in erythrocytes from controls (open bar) and patients (filled bar) incubated for 24 h in Ca^{2+}-containing (left column pair) or Ca^{2+}-free NaCl solution (right column pair). (**B**) Histogram showing the annexin V binding to erythrocytes from controls (black) and patients (red line) recorded by flow cytometry after 24h of incubation in Ca^{2+}-containing NaCl solution. (**C**) Mean percentage (±SEM; n=8-9) of phosphatidylserine-exposing erythrocytes (controls: open bar; patients: filled bar) as defined in (B) by the high annexin V binding (indicated by the marker). (**D**) Immunoblot showing calpain activation in Ca^{2+}-permeabilized (left lane) and patients' erythrocytes (right lane) but not in erythrocytes from controls (middle lane) following 24h incubation in Ca^{2+}-containing NaCl solution. Activation of calpain is indicated by the cleavage of the p80 pro-enzyme in its active p78 and p76 forms. (**E**) Mean percentage (± SEM; n=18) of erythrocytes (controls: open bar; patients: filled bar) that hemolyzed during 24 h of incubation in Ca^{2+}-containing NaCl solution
(*** $p<0.001$, two-tailed t-test (D, E) or ANOVA (A); n.s. not significantly different).

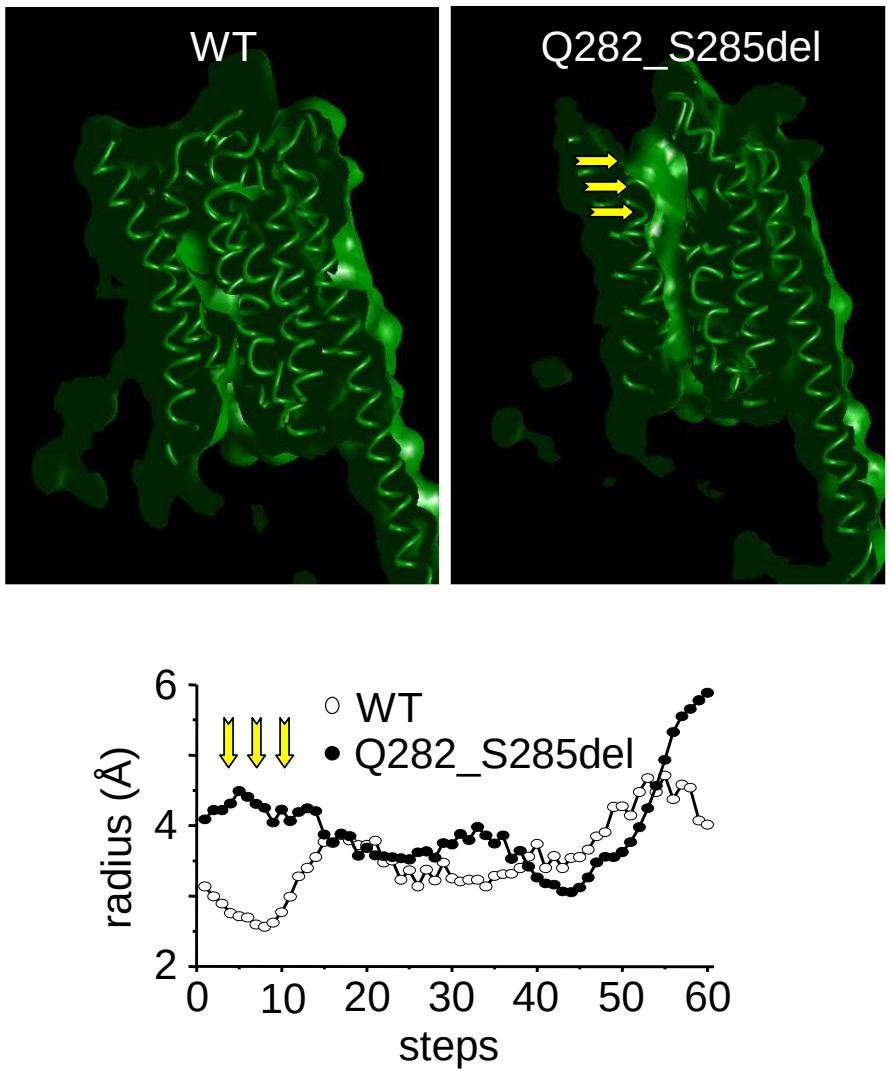

Figure S3. Molecular model of WT and mutant Q282_S285del GLUT1 transporters. We performed homology modeling using energy minimisation functions to generate an initial model for the mutation using the published coordinates of a GLUT1 model (ref. 22 of the main text). Comparison of the resulting two models suggested alterations in the outer diameter of the GLUT1 channel by the mutation. In order to determine the inner diameter of the central tunnel we used CAVER which detected one major tunnel. This tunnel has a considerably larger mouth opening in the mutant GLUT1 molecule (radius of about 4.1 Å) at the indicated position (yellow arrows) compared to the WT (radius of about 2.5 Å), which may allow entrance and passage of cations as shown by our functional assays.